Supporting Information

Sulfide-mediated growth of NIR Luminescent Pd/Ag atomically precise nanoclusters

Yu-Rong Ni,[a] Michael N. Pillay,[a] Tzu-Hao Chiu,[a] Hao Liang,[b] Samia Kahlal,[b] Jie-Ying Chen,[c] Yuan Jang Chen,[c] Jean-Yves Saillard,[b] and C. W. Liu*[a]*

Experimental

All chemicals, including palladium(II) acetate ($PdOAc_2$, 98%) and sodium borohydride ($NaBH_4$, 98%), were purchased commercially and used as received. $[Ag(CH_3CN)_4]PF_6$ and $NH_4[S_2P(OR)_2]$ (R = ^{i}Pr, ^{i}Bu) were made utilizing the method described in the literature.[S1,S2] NMR spectra were recorded on Bruker Advance II 400 and AVNEO-500 spectrometer , operating at 400 MHz for ^{1}H, 161.97 MHz for $^{31}P\{^1H\}$, 100 MHz for ^{13}C and 500 MHz for ^{1}H, 125 MHz for ^{13}C. ESI-MS and ESI-TOF-MS spectra were recorded on AB SCIE X QSTAR® XL High-Resolution Electrospray Mass spectrometer and a Fison Quattro Bio-Q (Fisons Instruments, VG Biotech, UK). The XPS spectra were recorded by using a PHI 5000 VersaProbe-Scanning ESCA Microprobe on an X-ray Photoelectron Spectrometer.

Optical measurement method

The optical absorption spectra were recorded using an Agilent Cary-60 spectrometer. Emission spectra and lifetime decays of complexes $\mathbf{1_{Pr}}$ and $\mathbf{1_{Bu}}$ were laser excited at 360 nm in an EPR tube equipped with a liquid nitrogen Dewar and collected on a HORIBA FluoroMax plus spectrometer. Emission spectra of $\mathbf{2_{Pr}}$ and $\mathbf{2_{Bu}}$ were excited by laser 532 nm and were recorded on a HORIBA JOBIN YVON iHR 550 spectrometer with two gratings (300 1/mm, 600 nm blaze in 298 K; 300 1/mm, 600 nm blaze in 77 K) and a HORIBA Symphony InGaZs-1700 detector with using the SynerJY software. Emission

lifetimes were collected using Hamamatsu NIR-PMT Modul H10330A-75 in the NIR region for compounds $\mathbf{2_{Pr}}$ and $\mathbf{2_{Bu}}$ at an excitation wavelength of 534 nm. A LeCroy WaveRunner 6030A is used to digitize the output data of the near-infrared detector system. The emission quantum yields of compounds $\mathbf{2_{Pr}}$ and $\mathbf{2_{Bu}}$ in 2-MeTHF solution were obtained by using $[Ru(bpy)_3]^{2+}$ as references in both ambient and low temperature.

SCXRD analysis

Paratone oil was used to coat the single crystals of **1**-**2**, which were then placed on a glass fiber. Data were gathered using a graphite mono-chromated Mo-Kα radiation source (λ=0.71073 Å) on a Brucker APEX II CCD diffractometer at 100 K. SADABS and SAINT adsorption corrections on raw data frames.[S3,S4] SHELXL-2018/3 package [S5,S6] integrated into SHELXL/PC V6.14. [S7] was used to solve the structure and then refined using least-squares versus F2.39,40 Anisotropic refinements were applied to all non-hydrogen atoms.

Computational Details

Geometry optimizations were performed by density functional theory (DFT) calculations with the Gaussian16 package,[S8] using the BP86 functional[S9,S10] and the Def2-TZVP basis set from EMSL Basis Set Exchange Library.[S11-S14] The Def2-ECP pseudopotential was applied for Pd.[S15] Relevant interatomic distances are provided in Table S2. The optimized geometries were characterized as true minima through vibrational analysis. The natural atomic orbital (NAO) charges and the Wiberg bond indices (WBI) were computed with the NBO6.0 program[S16] on single-point calculations performed with the BP86 functional and the Def2-SVP basis set [S11-S14] for computational limitations. The UV-visible transitions were calculated by means of time-dependent DFT (TD-DFT) calculations, with the CAM-B3LYP functional[S17] and the Def2-TZVP basis set, with solvent (THF) effect being considered within the PCM model[S18,S19] Only singlet-singlet, *i.e.* spin-allowed, transitions have been computed.

The UV-visible spectra were simulated from the computed TD-DFT transitions and their oscillator strengths by using the Multiwfn program,[S20] each transition being associated with a Gaussian function of half-height width equal to 3000 cm^{-1}. The compositions of the molecular orbitals were calculated using the AOMix program.[S21]

Synthesis

$[NH_4][S_2P(OR)_2]$ (0.307 mmol), Et_3N (100 µl, 0.717 mmol), and $Pd(OAc)_2$ (0.057 g, 0.256 mmol) were dissolved in 50 ml acetone at 253 K in a Schlenk reaction flask and stirred for 10 min. Then, $[Ag(CH_3CN)_4]PF_6$ (0.210/ g, 0.520 mmol) was added and stirred until the color changed from yellow to red. $NaBH_4$ (0.030 g, 0.801 mmol) was subsequently added and stirred for 12 hours. The solvent was removed in vacuo, and the residue extracted with dichloromethane DCM, and washed with DI water. The solution was subjected to thin-layer chromatography (TLC) with mixed solvent hexane and DCM (1:20) elution. The first band yielded a wheat color compound $[PdAg_{16}(S)_2\{S_2P(OR)_2\}_{12}]$ **1** (yield: 10.6 %) and the green compound $[Pd_6Ag_{14}(S)\{S_2P(OR)_2\}_{12}]$ **2** in 16.8 % yield (yield base on Pd).

$[PdAg_{16}(S)_2\{S_2P(O^iPr)_2\}_{12}]$, **$1_{Pr}$**: ^1H NMR (400 MHz, $CDCl_3$, δ, ppm, 298 K): 4.86 (septet, CH, 24H), 1.36 (d, CH_3, 144H). $^{31}P\{^1H\}$ NMR (161.97 MHz, $CDCl_3$, δ, ppm, 298 K): 105.31, 104.35 and 100.72. ESI-TOF-MS (*m/z*): exp. 4563.4390 (calc. 4563.4375 for $[\mathbf{1_{Pr}}+Ag]^+$). UV-Vis [λ_{max} in nm, (ε in $M^{-1}cm^{-1}$)]: 365 (56352). XPS (Calc.: Pd%0.78, Ag%12.59, S%20.47, P%9.44, C%56.70): Pd%0.61, Ag%10.30, S%18.03, P%10.71, C%60.36, and (binding energy, eV): Ag $3d_{5/2}$, 367.72; Ag $3d_{3/2}$, 373.72; Pd $3d_{5/2}$, 337.18; Pd $3d_{3/2}$, 342.34.

$[PdAg_{16}(S)_2\{S_2P(O^iBu)_2\}_{12}]$, **$1_{Bu}$**: ^1H NMR (400 MHz, $CDCl_3$, δ, ppm, 298 K): 3.92 (d, CH_2, 48H), 3.01(nonet, CH, 24H), 0.94(d, CH_3, 144H). $^{31}P\{^1H\}$ NMR (161.97 MHz, $CDCl_3$, δ, ppm, 298 K): 108.92, 106.27, 106.00, and 102.36. ESI-TOF-MS (*m/z*): exp. 4899.8438 (calc. 4899.8140 for $[\mathbf{1_{Bu}}+Ag]^+$). UV-Vis [λ_{max} in nm, (ε in $M^{-1}cm^{-1}$)]:366 (61386). XPS (Calc.: Pd%0.66, Ag%10.60,

S%17.22, P%7.94, C%63.58): Pd%1.13, Ag%10.10, S%14.07, P%7.80, C%66.89, and (binding energy, eV): Ag $3d_{5/2}$, 367.62; Ag $3d_{3/2}$, 373.62; Pd $3d_{5/2}$, 337.03; Pd $3d_{3/2}$, 342.30. Elemental analysis (Calc.: C%23.86, H%4.44, S%17.54): C%24.06, H%4.54, 17.39.

$[Pd_6Ag_{14}(S)\{S_2P(O^iBu)_2\}_{12}]$, **$2_{Bu}$**: ^1H NMR (400 MHz, $CDCl_3$, δ, ppm, 298 K): 3.87 (d, CH_2, 48H), 2.01(nonet, CH, 24H), 0.97(d, CH_3, 144H). $^{31}P\{^1H\}$ NMR (161.97 MHz, $CDCl_3$, δ, ppm, 298 K): 102.63, 1000.58. ESI-TOF-MS (*m/z*): exp. 5184.6678(calc. 5184.5506 for $[\mathbf{2_{Bu}}+Ag]^+$). UV-Vis [λ_{max} in nm, (ε in $M^{-1}cm^{-1}$)]:374 (40816), 413(42346), 446 (40840), 545 (26921), 625 (25381). XPS (Calc.: Pd%3.92, Ag%9.15, S%16.34, P%7.84, C%62.75): Pd%3.62, Ag%7.93, S%14.80, P%8.02, C%65.63, and (binding energy, eV): Ag $3d_{5/2}$, 367.48; Ag $3d_{3/2}$, 373.48; Pd $3d_{5/2}$, 335.58; Pd $3d_{3/2}$, 340.96. Elemental analysis (Calc.: C%23.13, H%4.40, S%15.82): C%22.71, H%4.29, 15.82.

References

[S1] A. A. M. Aly, B. Walfort, H. Lang, *Kristallogr. NCS*, **2004**, *219*, 521–523.

[S2] V. P. Wystrach, E. O. Hook, G. L. M. Christpoher, *J. Org. Chem.*, **1956**, *21*, 705–707.

[S3] SADABS, version 2014-11.0, Bruker Area Detector Absorption Correxions (Bruker AXS Inc., Madison, WI, 2014).

[S4] SAINT, included in G. Jogl, V4.043: Software for the CCD detector system (Bruker Analytical: Madison, WI, 1995). S5.

[S5] G. M. Sheldrick, *Acta Cryst. A,* **2008**, *64*, 112-122.

[S6] T. Gruene, H. W. Hahn, A. V. Luebben, F. Meilleur, G. M. J. Sheldrick, Appl. Cryst. **2014**, *47*, 462-466.

[S7] SHELXTL, version 6.14. (Bruker AXS Inc., Madison, Wisconsin, USA, 2003).

[S8] Gaussian 16, Revision B.01, M. J. Frisch, G. W. Trucks, H. B. Schlegel, G. E. Scuseria, M. A. Robb, J. R. Cheeseman, G. Scalmani, V. Barone, G. A. Petersson, H. Nakatsuji, X. Li, M. Caricato, A. V. Marenich, J. Bloino, B. G. Janesko, R. Gomperts, B. Mennucci, H. P. Hratchian, J. V. Ortiz, A. F. Izmaylov, J. L. Sonnenberg, D. Williams-Young, F. Ding, F. Lipparini, F. Egidi, J. Goings, B. Peng, A. Petrone, T. Henderson, D. Ranasinghe, V. G. Zakrzewski, J. Gao, N. Rega, G. Zheng, W. Liang, M. Hada, M. Ehara, K. Toyota, R. Fukuda, J. Hasegawa, M. Ishida, T. Nakajima, Y. Honda, O. Kitao, H. Nakai, T. Vreven, K. Throssell, J. A. Montgomery, Jr., J. E. Peralta, F. Ogliaro, M. J. Bearpark, J. J. Heyd, E. N. Brothers, K.

N. Kudin, V. N. Staroverov, T. A. Keith, R. Kobayashi, J. Normand, K. Raghavachari, A. P. Rendell, J. C. Burant, S. S. Iyengar, J. Tomasi, M. Cossi, J. M. Millam, M. Klene, C. Adamo, R. Cammi, J. W. Ochterski, R. L. Martin, K. Morokuma, O. Farkas, J. B. Foresman, D. J. Fox, Gaussian, Inc., Wallingford CT, 2016.

[S9] A. D. Becke, *Phys. Rev. A*, **1988**, *38*, 3098-3100;

[S10] J. P. Perdew, *Phys. Rev. B*, **1986**, *33*, 8822-8824.

[S11] A. Schaefer, H. Horn, R. Ahlrichs, *J. Chem. Phys.,* **1992**, *97,* 2571-77.

[S12] A. Schaefer, C. Huber, R. Ahlrichs, *J. Chem. Phys.,* **1994**, *100*, 5829-5835.

[S13] F. Weigend, R. Ahlrichs, *Phys. Chem. Chem. Phys*. **2005**, *7*, 3297-3305.

[S14] F. Weigend, *Phys. Chem. Chem. Phys.,* **2006**, *8,* 1057-1065.

[S15] D. Andrae, U. Häussermann, M. Dold, H. Stoll, H. Preuss, *Theor. Chim. Acta*, **1990**, *77*, 123-141.

[S16] E. D. Glendening, J. K. Badenhoop, A. E. Reed, J. E. Carpenter, J. A. Bohmann, C. M. Morales, C. R. Landis, F. Weinhold, *NBO 6.0*; Theoretical Chemistry Institute, University of Wisconsin, Madison, WI, 2013**,** http://nbo6.chem.wisc.edu.

[S17] T. Yanai, D. Tew, N. Handy, *Chem. Phys. Lett.,* **2004**, *393*, 51-57.

[S18] M. Cossi, V. Barone, R. Cammi, J. Tomasi, *Chem. Phys. Lett.* **1996**, *255*, 327-335

[S19] V. Barone, M. Cossi, J. Tomasi, *J. Chem. Phys.,* **1997**, *107*, 3210-3221.

[S20] T. Lu, F. Chen, *J. Comput. Chem*. **2012**, *33*, 580-592.

[S21] S. I. Gorelsky, A. B. P. Lever, *J. Organomet. Chem*. **2001**, *635*, 187-196.

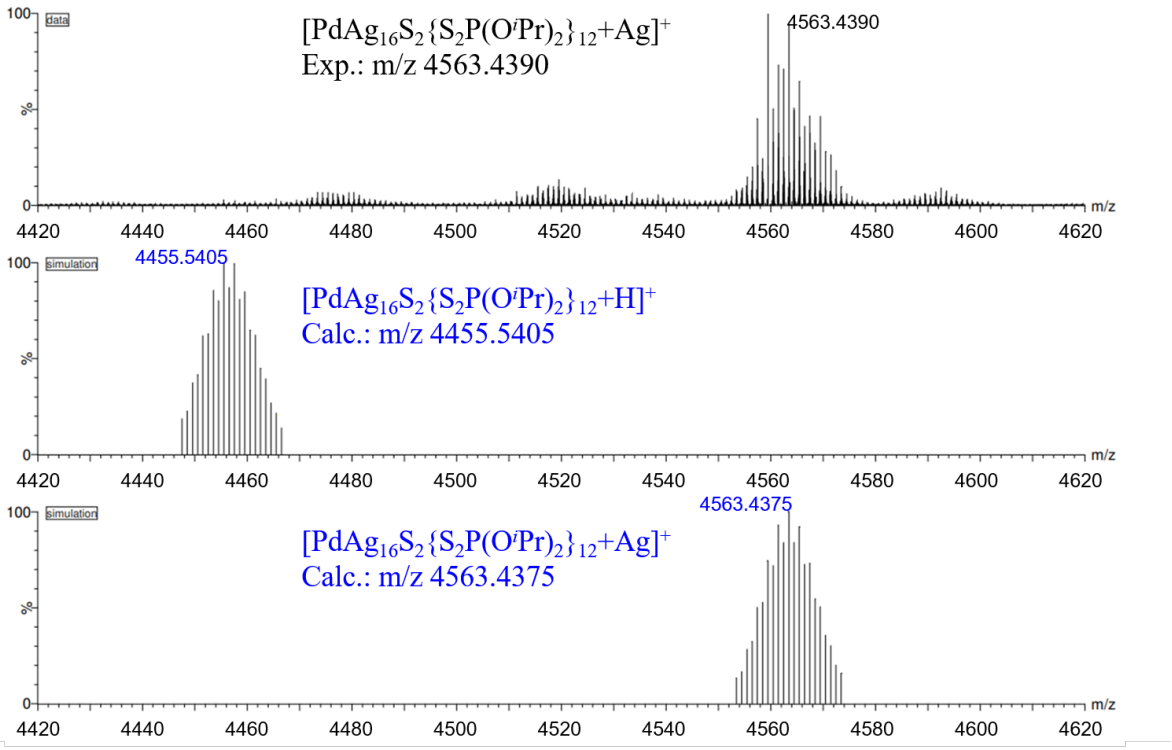

Figure S1. ESI-TOF-MS spectra of $\mathbf{1_{Pr}}$ with experimental (black) and simulated (blue) data, assigned to a silver and proton adduct.

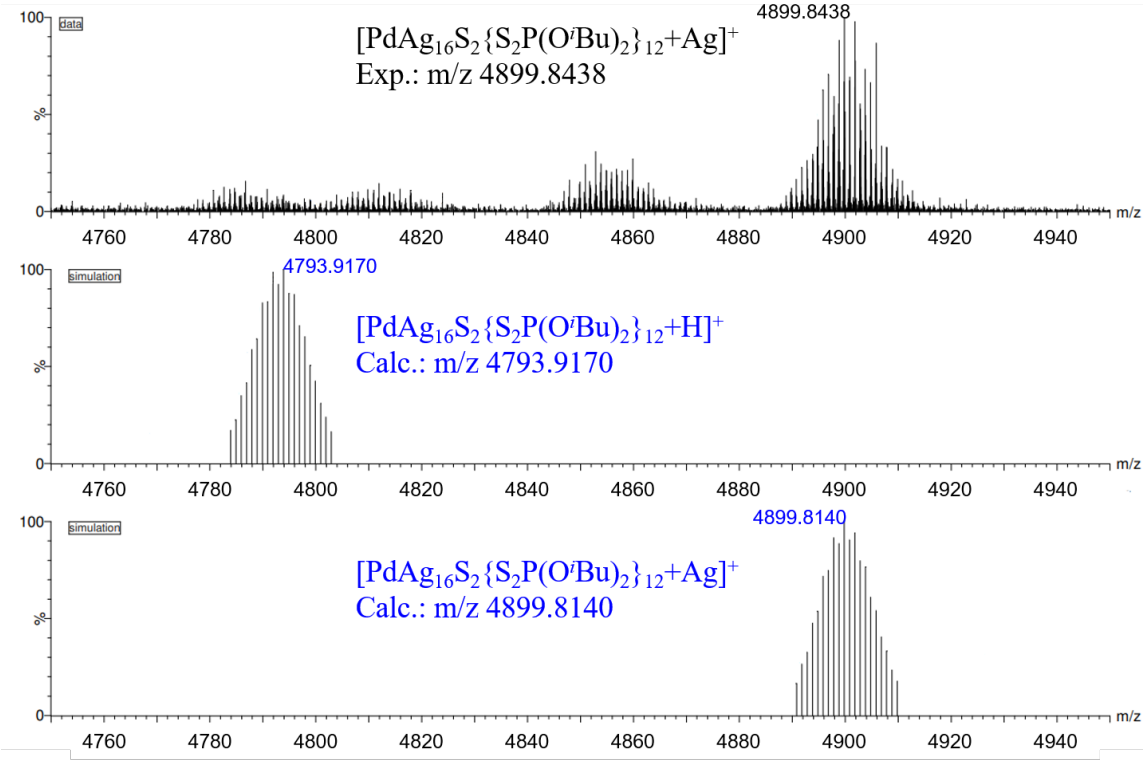

Figure S2. ESI-TOF-MS spectra of $\mathbf{1_{Bu}}$ with experimental (black) and simulated (blue) data, assigned to a silver and proton adduct.

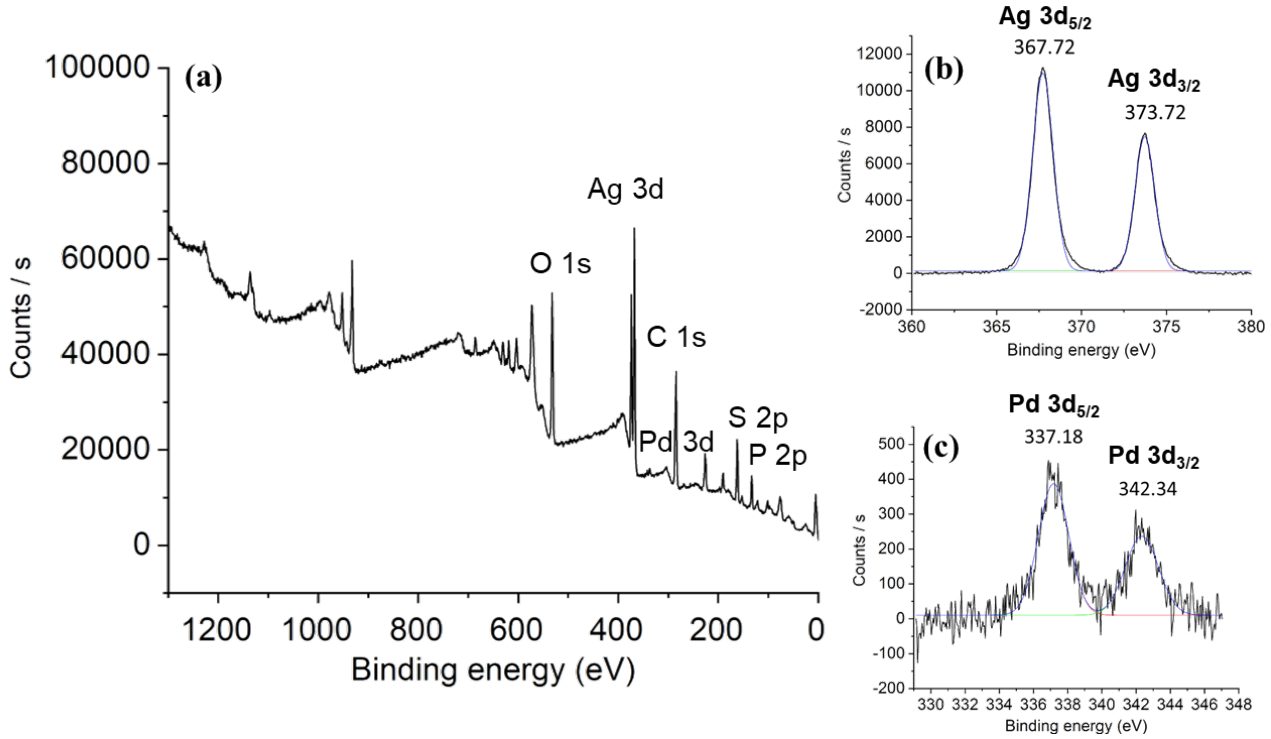

Figure S3. (a) XPS analysis of $\mathbf{1}_{Pr}$. (b) The Ag 3d spectrum of $\mathbf{1}_{Pr}$. (c) The Pd 3d spectrum of $\mathbf{1}_{Pr}$.

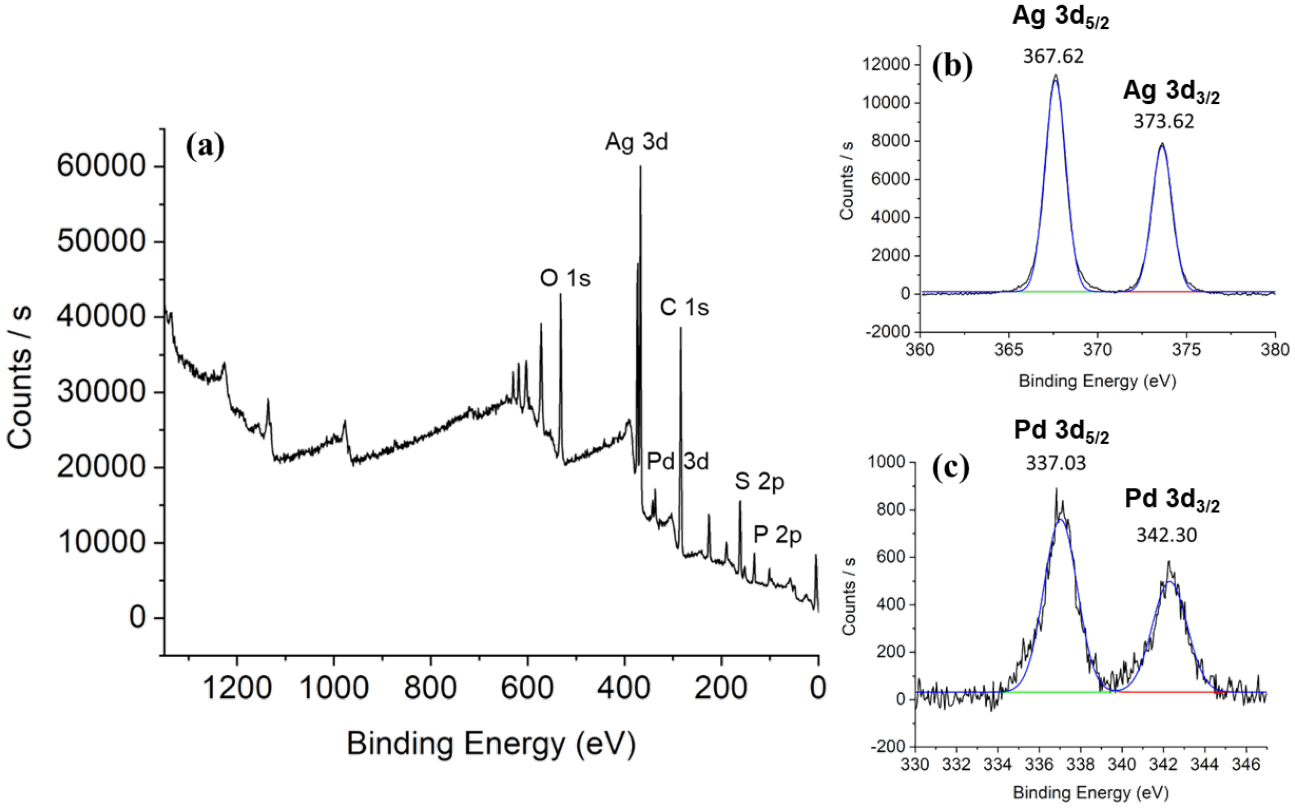

Figure S4. (a) XPS analysis of $\mathbf{1}_{Bu}$. (b) The Ag 3d spectrum of $\mathbf{1}_{Bu}$. (c) The Pd 3d spectrum of $\mathbf{1}_{Bu}$.

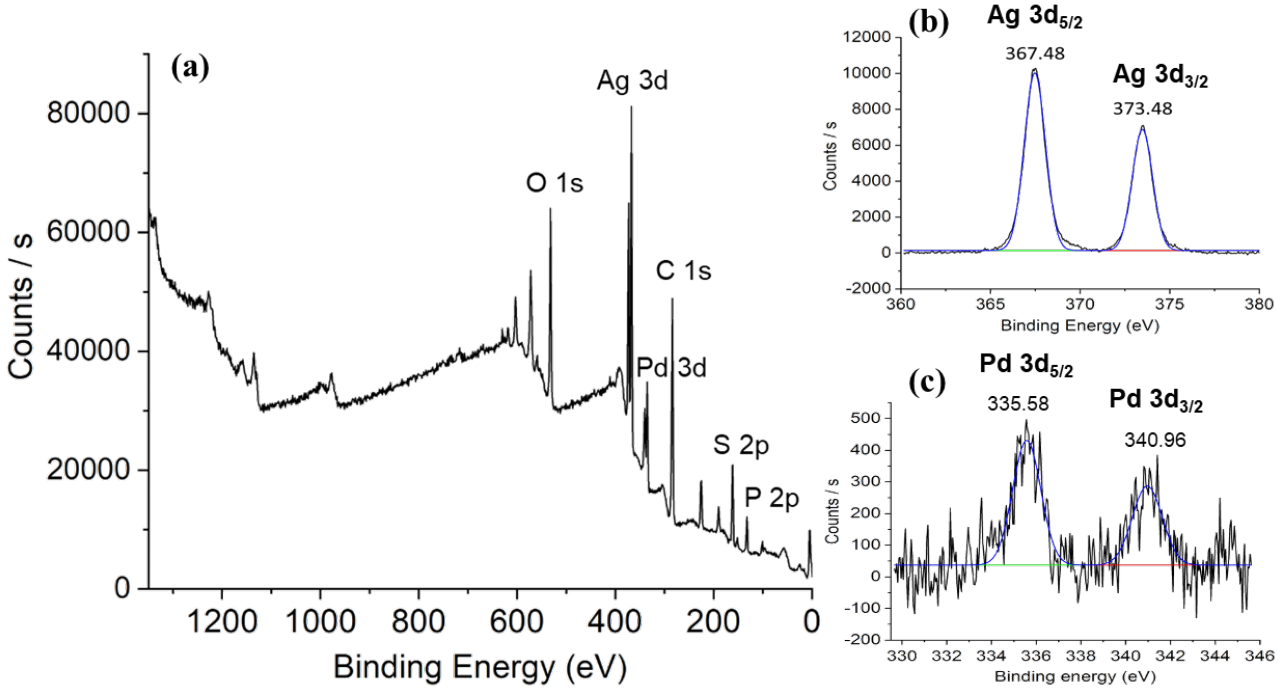

Figure S5. (a) XPS analysis of $\mathbf{2}_{\mathbf{Bu}}$. (b) The Ag 3d spectrum of $\mathbf{2}_{\mathbf{Bu}}$. (c) The Pd 3d spectrum of $\mathbf{2}_{\mathbf{Bu}}$.

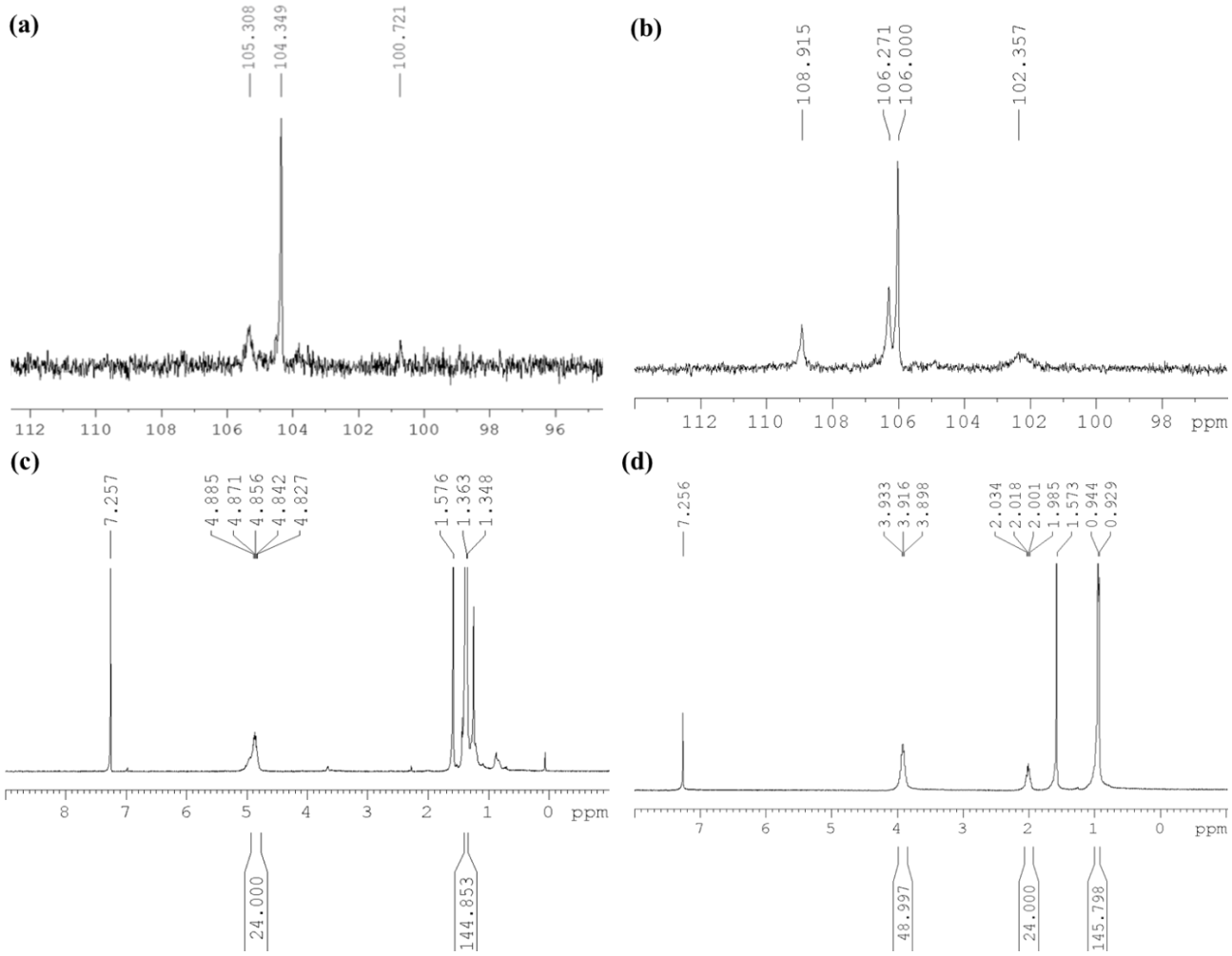

Figure S6. ^{31}P NMR spectrum (161.97 MHz) of (a) $\mathbf{1_{Pr}}$, (b) $\mathbf{1_{Bu}}$ and ^{1}H NMR spectra (400 MHz) of (c) $\mathbf{1_{Pr}}$, (d) $\mathbf{1_{Bu}}$ in $CDCl_3$.

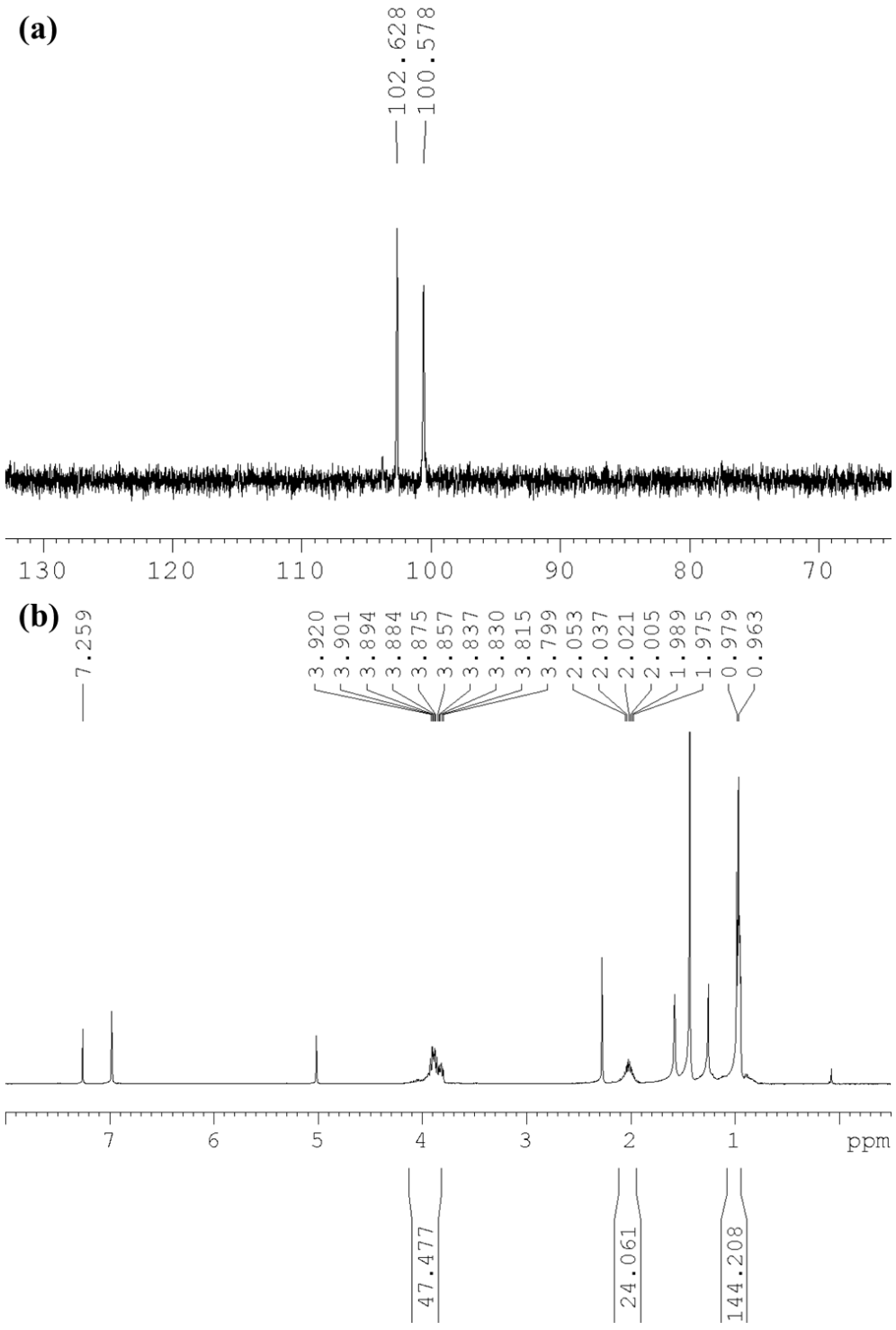

Figure S7. (a) ^{31}H NMR spectrum (161.97 MHz) of $\mathbf{2_{Bu}}$. (d) ^{1}H NMR spectra (400 MHz) of $\mathbf{2_{Bu}}$ in $CDCl_3$.

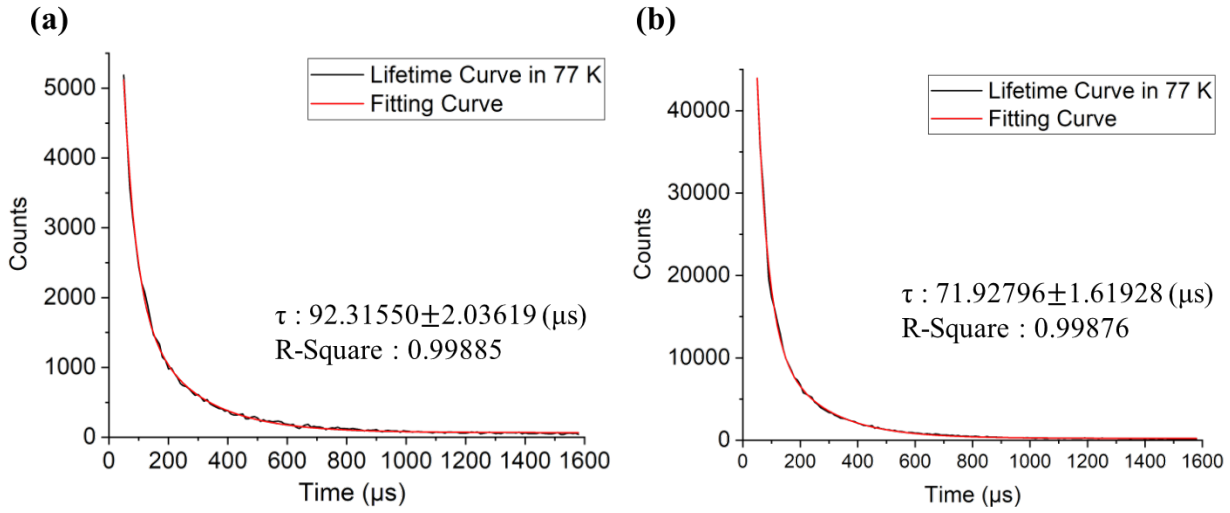

Figure S8. Time-resolved photoluminescence spectrum of (a) $\mathbf{1}_{Pr}$, (b) $\mathbf{1}_{Bu}$, and in 2Me-THF at 77 K.

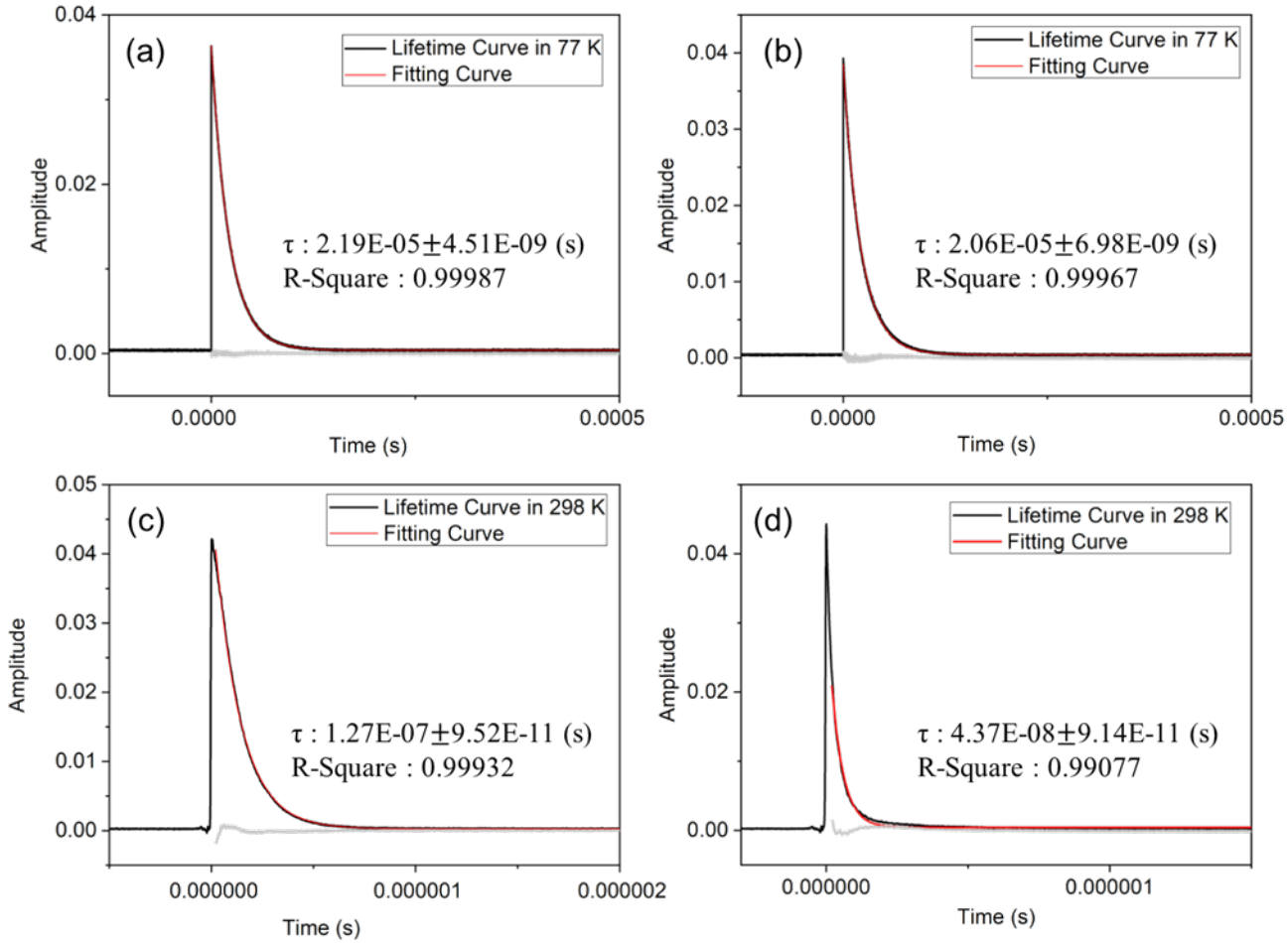

Figure S9. Time-resolved photoluminescence spectrum in 2Me-THF of (a) $\mathbf{2}_{Pr}$ and (b) $\mathbf{2}_{Bu}$ at 77 K; (c) $\mathbf{2}_{Pr}$ and (d) $\mathbf{2}_{Bu}$ at 298 K.

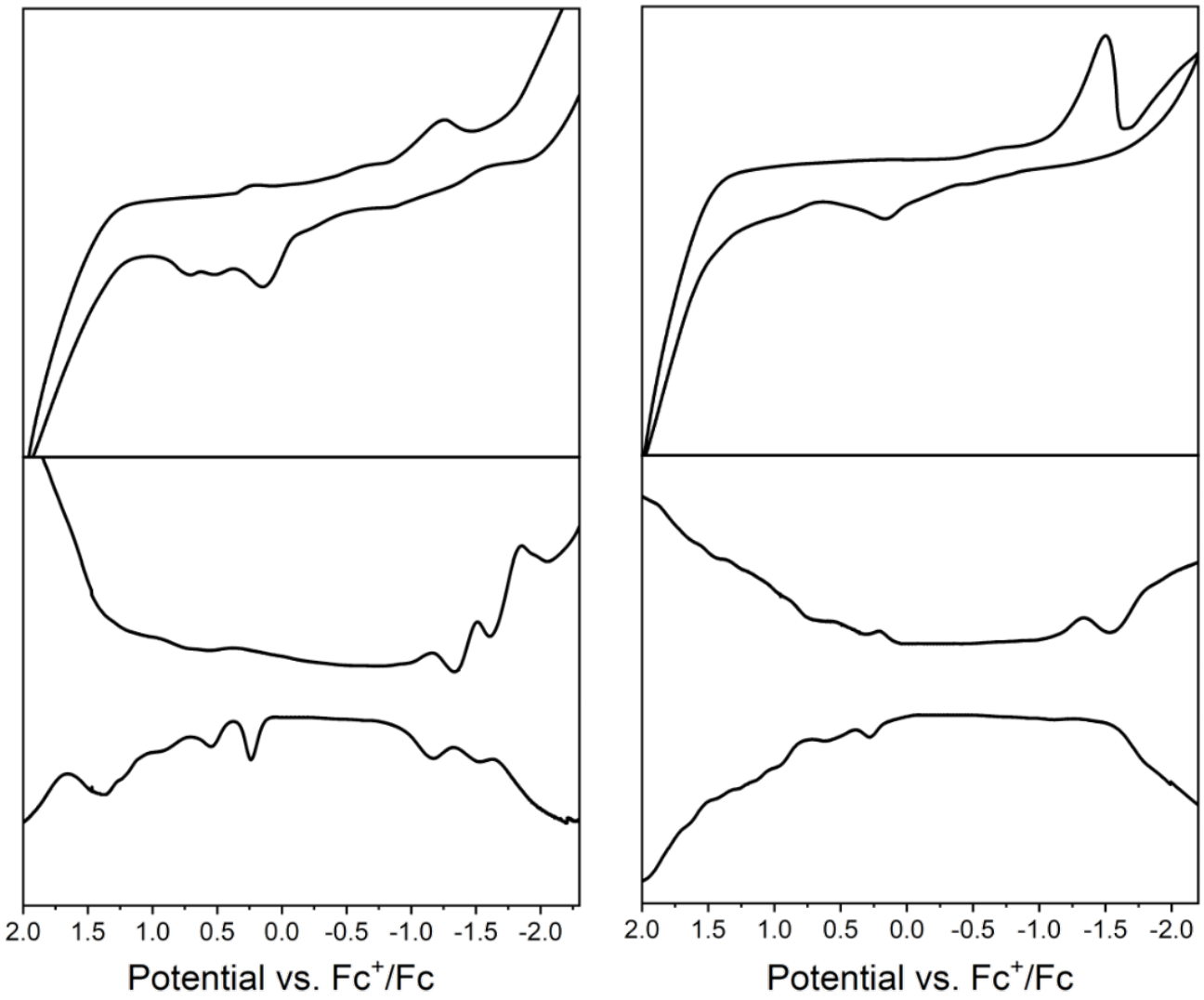

Figure S10. Cyclic voltammogram (a) at 298 K, (b) at 233 K of $\mathbf{1_{Pr}}$ recorded in CH_2Cl_2. Square wave voltammogram (c) at 298 K, (d) at 233 K of $\mathbf{1_{Pr}}$ recorded in CH_2Cl_2.

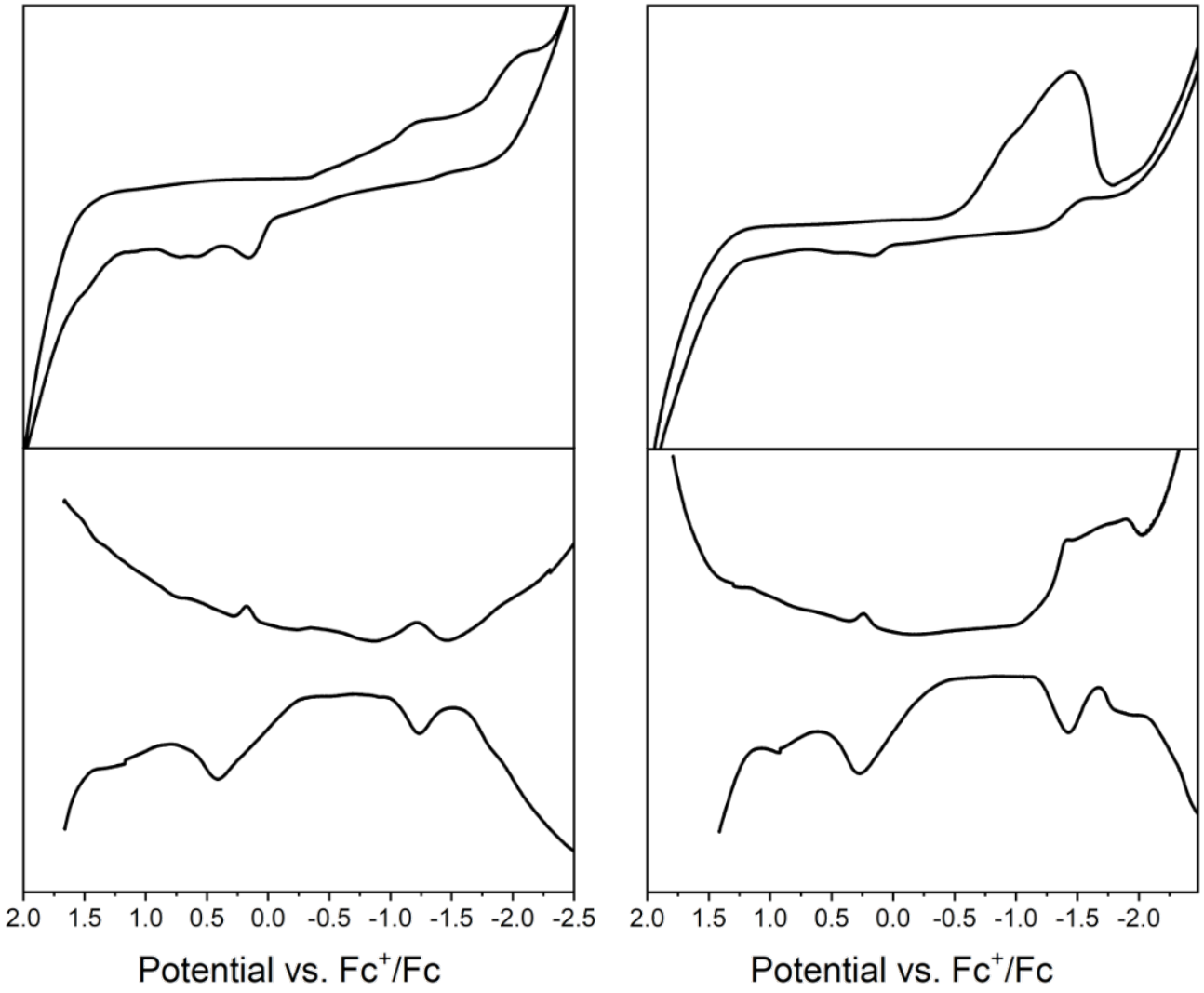

Figure S11. Cyclic voltammogram (a) at 298 K, (b) at 233 K of $\mathbf{1_{Bu}}$ recorded in CH_2Cl_2. Square wave voltammogram (c) at 298 K, (d) at 233 K of $\mathbf{1_{Bu}}$ recorded in CH_2Cl_2.

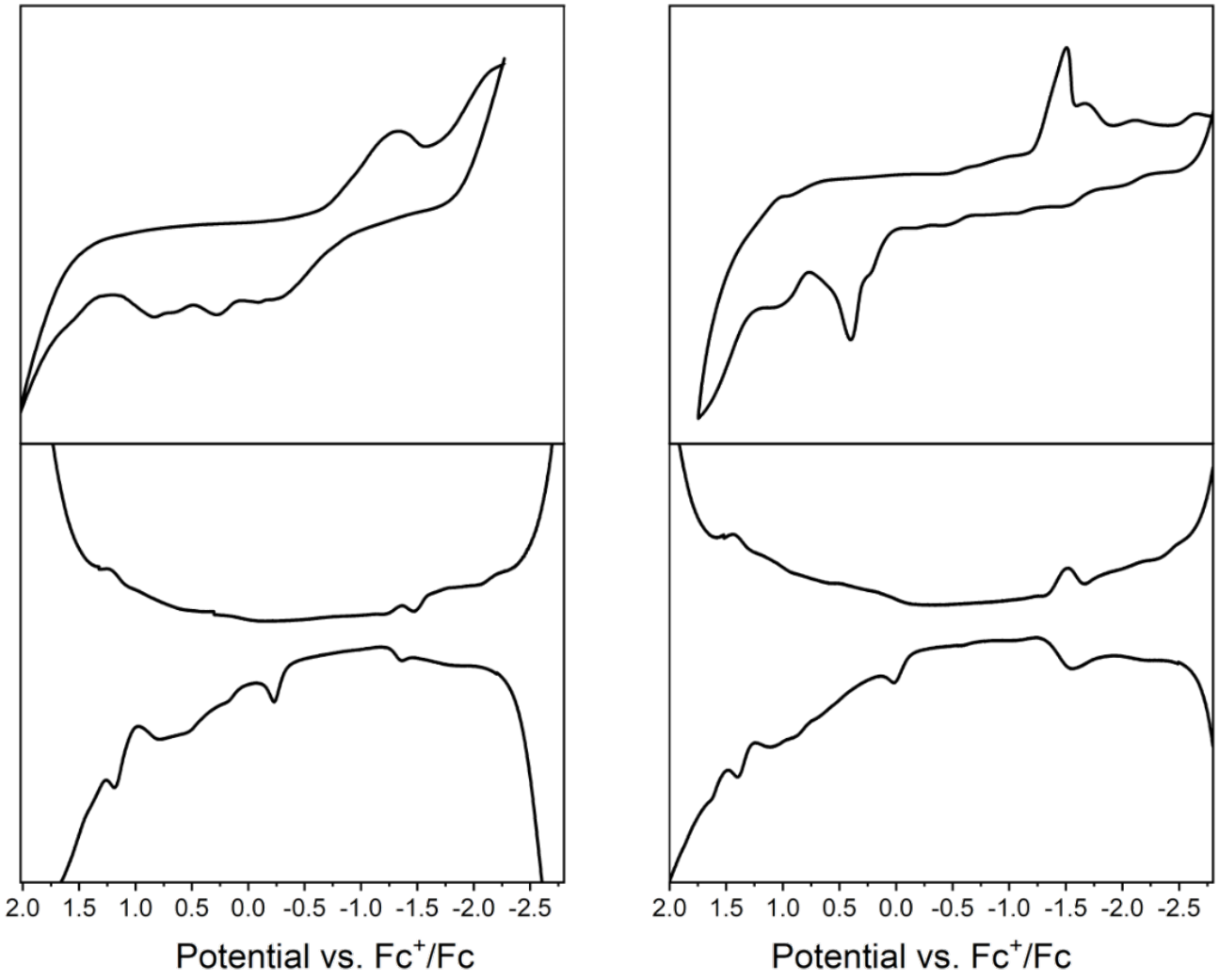

Figure S12. Cyclic voltammogram (a) at 298 K, (b) at 233 K of $\mathbf{2_{Bu}}$ recorded in CH_2Cl_2. Square wave voltammogram (c) at 298 K, (d) at 233 K of $\mathbf{2_{Bu}}$ recorded in CH_2Cl_2.

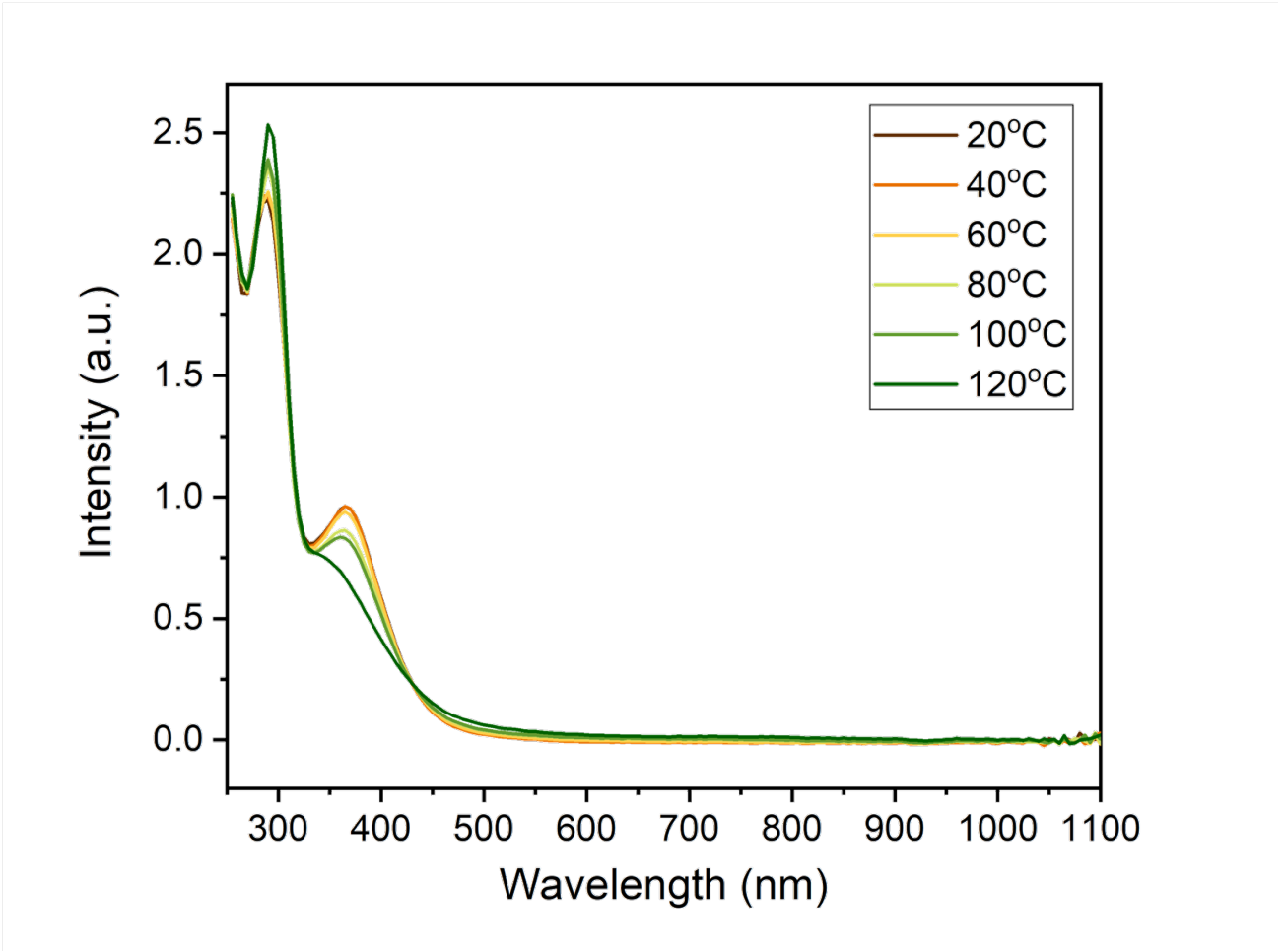

Figure S13. The temperature-dependent UV-vis spectrum of $\mathbf{1}_{Pr}$ in DMF.

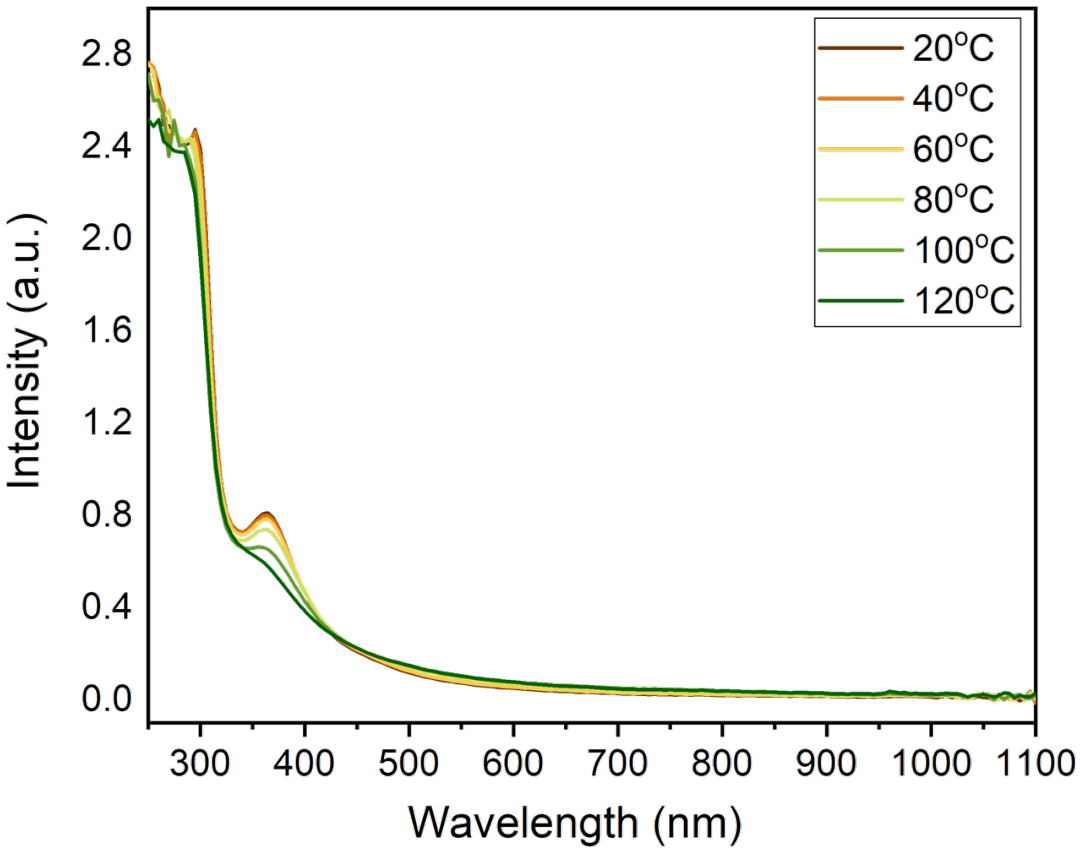

Figure S14. The temperature-dependent UV-vis spectrum of $\mathbf{1_{Bu}}$ in DMF.

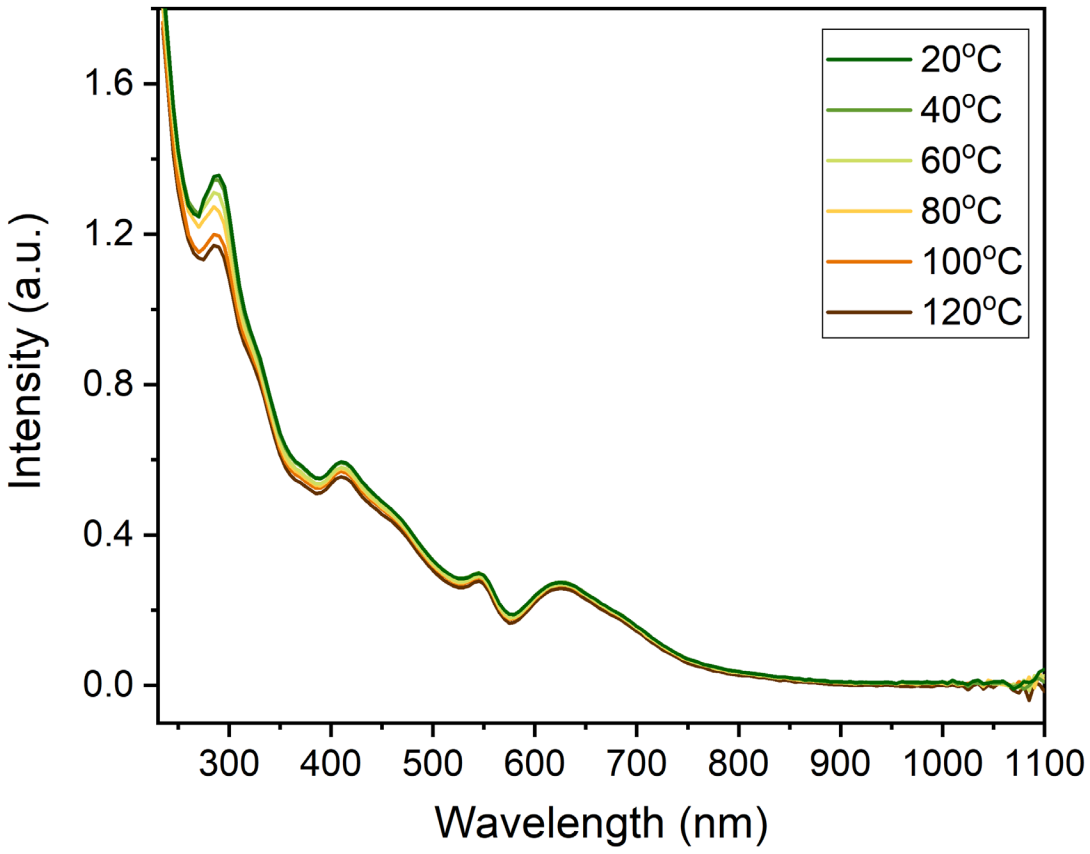

Figure S15. The temperature-dependent UV-vis spectrum of $\mathbf{2_{Bu}}$ in DMF.

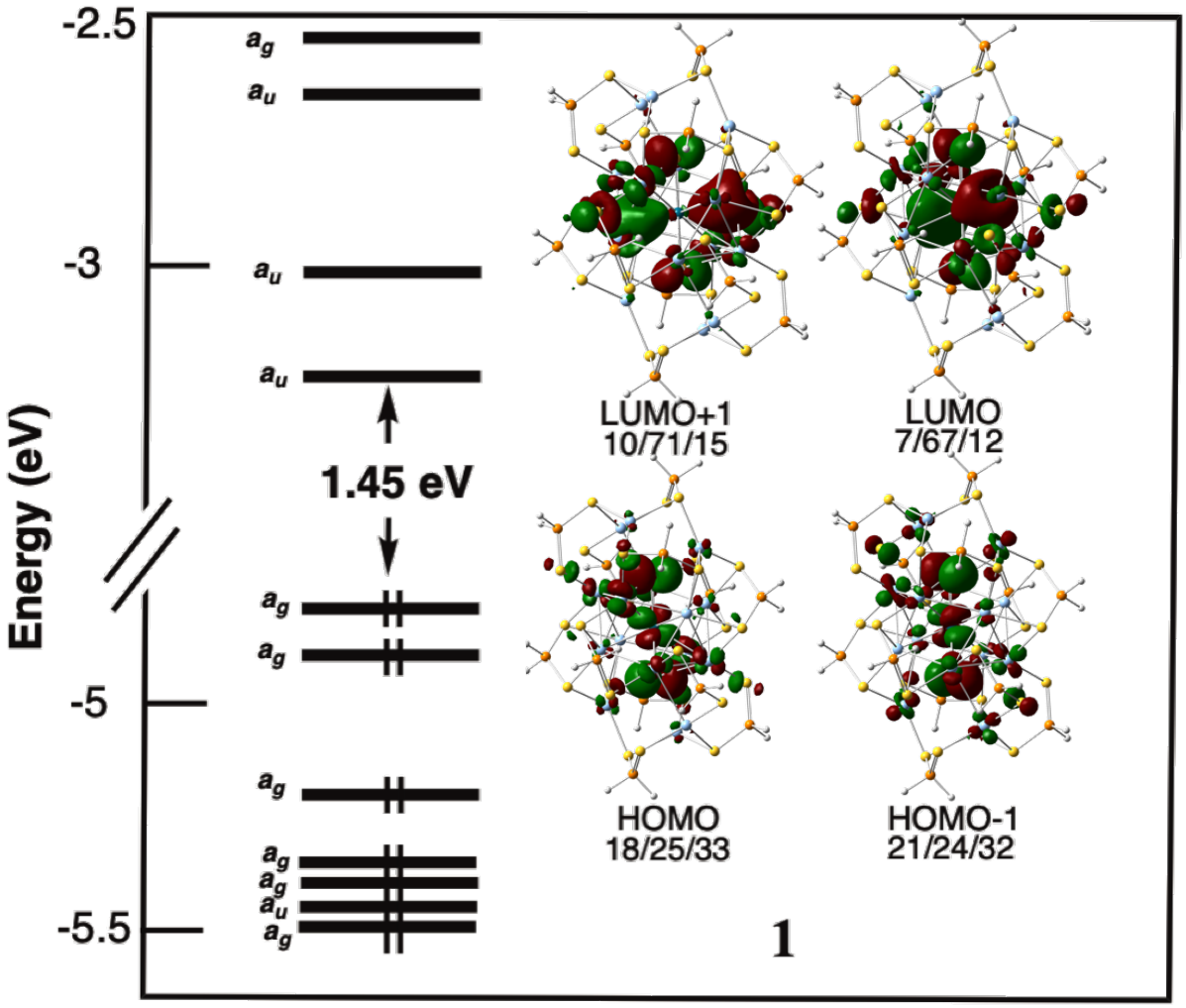

Figure S16. The Kohn-Sham MO diagram of **1**. Orbital localization (%) are given in the order Pd/Ag/$S_{sulfide}$.

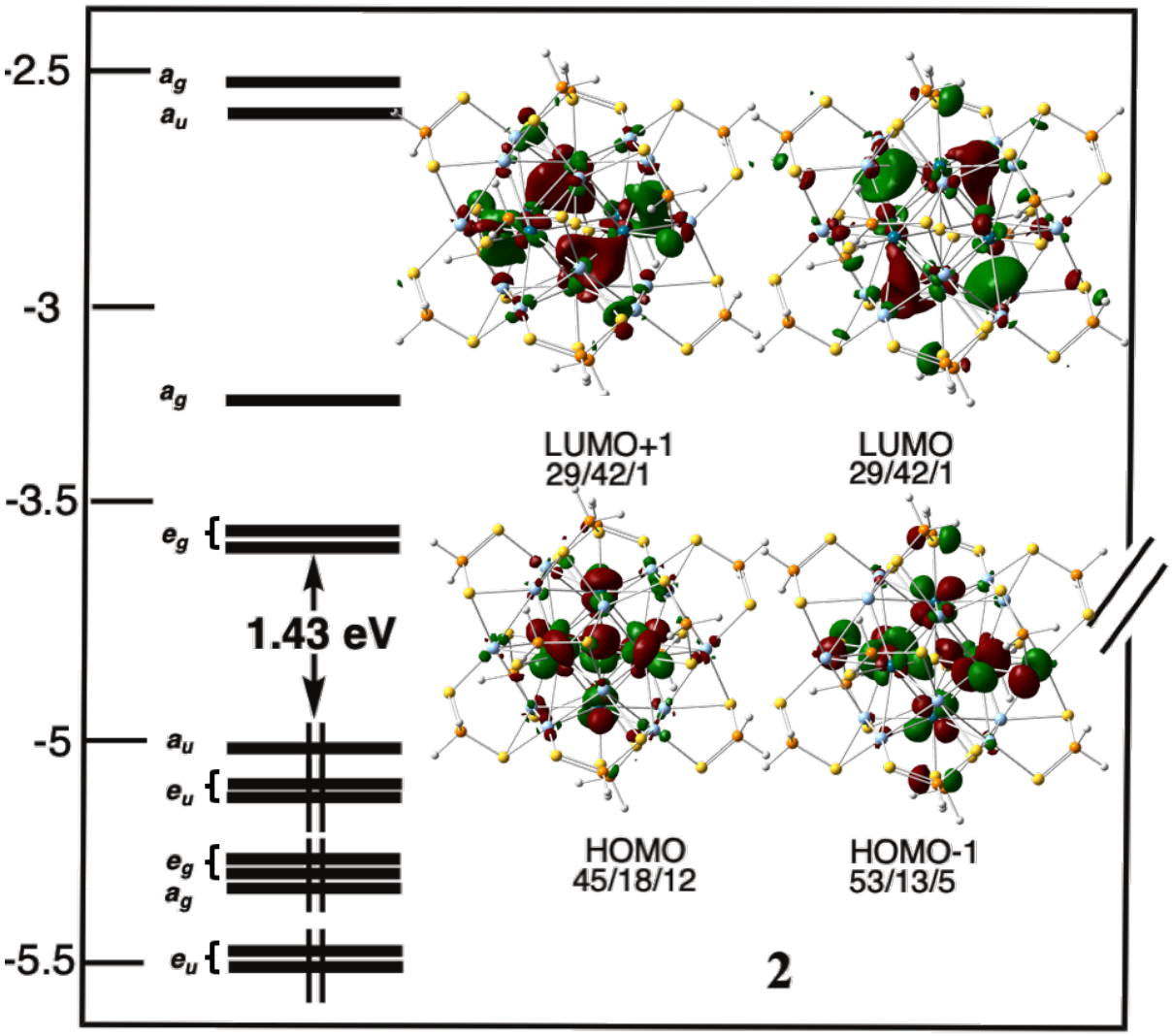

Figure S17. The Kohn-Sham MO diagram of **2**. Orbital localization (%) are given in the order Pd/Ag/$S_{sulfide}$.

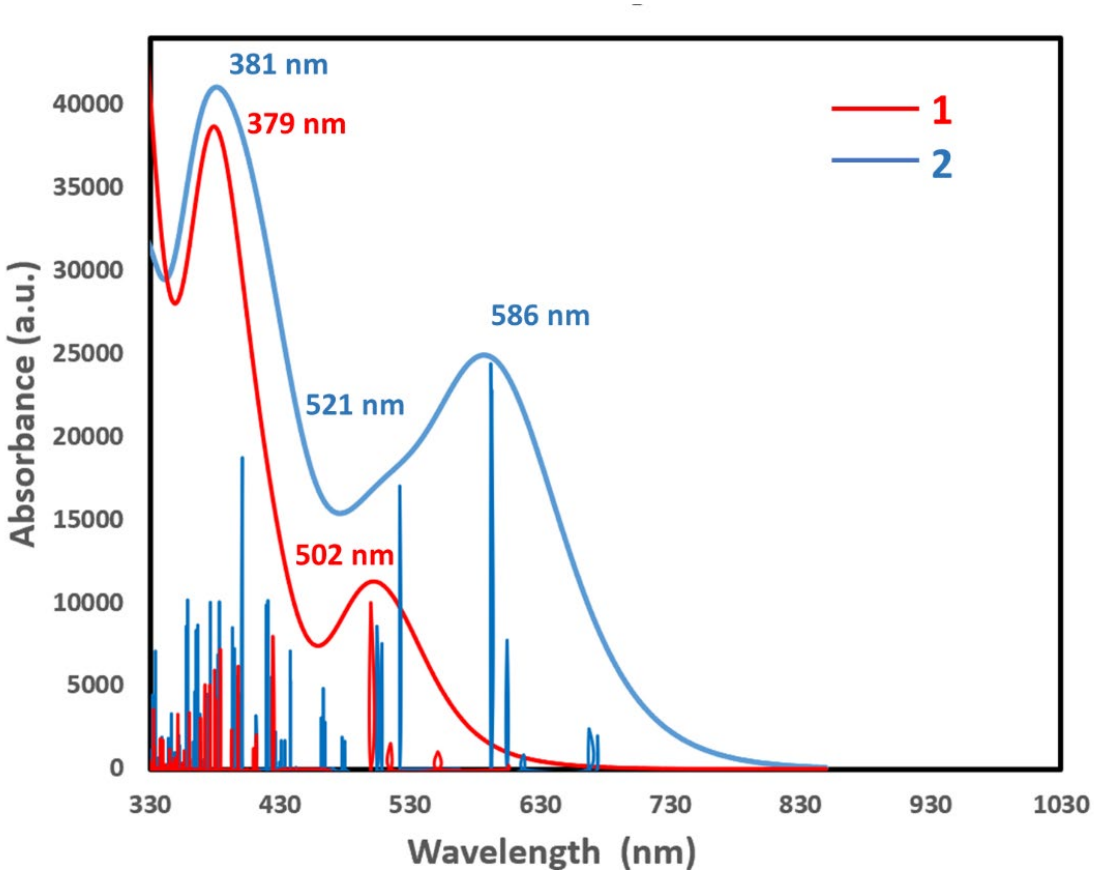

Figure S18. The TD-DFT simulated spectra of **1** and **2**. Vertical bars correspond to the computed transitions of heights proportional to their oscillator strength.

Table S1. Crystallographic data and refinement details of $\mathbf{1_{Pr}}$, $\mathbf{1_{Bu}}$, and $\mathbf{2_{Bu}}$.

	$\mathbf{1_{Pr}}$ (CCDC: 2379720)	$\mathbf{1_{Bu}}$ (2379721)	**2** (2379722)
Chemical formula	$C_{74}H_{172}Ag_{16}Cl_4O_{24}P_{12}PdS_{26}$	$C_{96}H_{216}Ag_{16}O_{24}P_{12}PdS_{26}$	$C_{96}H_{216}Ag_{14}O_{24}P_{12}Pd_6S_{25}$
M_r	4625.43	4792.19	5076.40
Crystal system, space group	Monoclinic, $P2_1/n$	Orthorhombic, $Pccn$	Triclinic, $P\bar{1}$
Temperature (K)	100	100	296
a, b, c (Å)	18.2605 (7), 21.6169 (8), 18.9717 (7)	26.454 (3), 27.073 (3), 23.350 (3)	15.605 (5), 18.060 (5), 18.102 (8)
α, β, γ (°)	90, 96.372 (1), 90	90, 90, 90	119.776 (6), 93.951 (10), 103.556 (7)
V (Å^3)	7442.5 (5)	16723 (4)	4200 (3)
Z	2	4	1
Radiation type	Mo $K\alpha$	Mo $K\alpha$	Mo $K\alpha$
μ (mm^{-1})	2.79	2.42	2.69
Crystal size (mm)	0.30 × 0.25 × 0.10	0.15 × 0.09 × 0.09	0.19 × 0.17 × 0.13
T_{min}, T_{max}	0.604, 0.746	0.553, 0.746	0.621, 0.745
Measured, independent and observed [$I > 2\sigma(I)$] reflections	57603, 18453, 16312	138769, 14719, 13322	48336, 14786, 9005
R_{int}	0.021	0.071	0.031
$(\sin\theta/\lambda)_{max}$ (Å^{-1})	0.667	0.595	0.595
$R[F^2 > 2\sigma(F^2)]$, $wR(F^2)$, S	0.031, 0.081, 1.05	0.081, 0.170, 1.36	0.065, 0.231, 1.07
No. of reflections	18453	14719	14786
No. of parameters	794	831	800
No. of restraints	328	323	518
	$w = 1/[\sigma^2(F_o^2) + (0.0302P)^2 + 30.7193P]$ where $P = (F_o^2 + 2F_c^2)/3$	$w = 1/[\sigma^2(F_o^2) + 518.3701P]$ where $P = (F_o^2 + 2F_c^2)/3$	$w = 1/[\sigma^2(F_o^2) + (0.0976P)^2 + 19.1642P]$ where $P = (F_o^2 + 2F_c^2)/3$
$\Delta\rho_{max}$, $\Delta\rho_{min}$ (e Å^{-3})	2.57, −2.00	1.81, −1.29	1.11, −0.72

Table S2. Relevant DFT-computed natural atomic orbital (NAO) charges.

Atom Type	**1**	**2**
Pd	-0.38	-0.34
Ag_{ker}	0.54-0.61 avg. 0.58	0.71
Ag_{cap}	0.64-0.68 avg. 0.66	0.63-0.71 avg. 0.67
$S_{sulfide}$	-1.09	-0.58

Optimized geometries for **1** and **2**. (.xyz file)

79

Compound 1

Pd	0.000000	0.000000	0.000000
Ag	2.263877	1.255977	1.188466
Ag	1.186102	-1.389321	2.374275
Ag	-1.779875	-1.890893	1.694087
Ag	-2.725104	0.897642	0.795192
Ag	-0.625580	2.777163	0.062796
Ag	0.625580	-2.777163	-0.062796
Ag	-2.263877	-1.255977	-1.188466
Ag	-1.186102	1.389321	-2.374275
Ag	1.779875	1.890893	-1.694087
Ag	2.725104	-0.897642	-0.795192
Ag	0.616866	2.831169	3.447239
Ag	-0.226914	0.035646	5.396634
Ag	-3.289004	0.104538	3.804981
Ag	-0.616866	-2.831169	-3.447239
Ag	0.226914	-0.035646	-5.396634
Ag	3.289004	-0.104538	-3.804981
S	-0.587608	0.477607	2.209445
S	0.587608	-0.477607	-2.209445
S	0.079396	4.594426	1.712105
S	3.024799	3.534627	-0.018188
S	-0.292343	2.536572	5.803691
S	-3.535911	2.538174	4.287082
S	3.098370	2.100708	3.527262
S	1.987702	-1.013068	4.920072
S	2.066880	-3.756400	2.054405
S	3.637098	-3.374947	-1.043254
S	-2.366543	-1.131005	5.912939
S	-1.087788	-3.551047	3.628269
S	-4.724165	-1.549864	2.585922
S	-4.731541	-0.017930	-0.597654
S	-0.079396	-4.594426	-1.712105

S	-3.024799	-3.534627	0.018188
S	0.292343	-2.536572	-5.803691
S	3.535911	-2.538174	-4.287082
S	-3.098370	-2.100708	-3.527262
S	-1.987702	1.013068	-4.920072
S	-2.066880	3.756400	-2.054405
S	-3.637098	3.374947	1.043254
S	2.366543	1.131005	-5.912939
S	1.087788	3.551047	-3.628269
S	4.724165	1.549864	-2.585922
S	4.731541	0.017930	0.597654
P	1.793805	4.984629	0.673676
P	-2.320747	2.879813	5.841445
P	3.228525	0.596780	4.887221
P	3.781136	-3.665596	0.934042
P	-2.172173	-3.059453	5.229727
P	-5.667237	-0.493127	1.139162
P	-1.793805	-4.984629	-0.673676
P	2.320747	-2.879813	-5.841445
P	-3.228525	-0.596780	-4.887221
P	-3.781136	3.665596	-0.934042
P	2.172173	3.059453	-5.229727
P	5.667237	0.493127	-1.139162
H	2.593023	5.869530	1.447188
H	1.399174	5.825770	-0.400132
H	-2.473988	4.246042	6.197750
H	-2.770931	2.229371	7.022822
H	4.551291	0.086697	4.802095
H	3.235932	1.178611	6.182972
H	4.664331	-2.722009	1.529204
H	4.453420	-4.889280	1.199008
H	-1.709623	-3.823550	6.335029
H	-3.510037	-3.526775	5.112563
H	-6.217828	0.693801	1.692004

H	-6.839004	-1.220014	0.794648
H	-4.664331	2.722009	-1.529204
H	-4.453420	4.889280	-1.199008
H	6.217828	-0.693801	-1.692004
H	6.839004	1.220014	-0.794648
H	-2.593023	-5.869530	-1.447188
H	-1.399174	-5.825770	0.400132
H	2.473988	-4.246042	-6.197750
H	2.770931	-2.229371	-7.022822
H	-4.551291	-0.086697	-4.802095
H	-3.235932	-1.178611	-6.182972
H	1.709623	3.823550	-6.335029
H	3.510037	3.526775	-5.112563

81

Compound 2

Ag	-0.41487	-4.27826	0.06021
Ag	1.29939	-2.83022	2.0177
Pd	-1.1809	-1.64233	1.09702
Ag	-0.0021	-0.00105	3.31577
Pd	2.01182	-0.20188	1.09866
Ag	1.8009	2.54032	2.01628
Pd	-0.83197	1.84327	1.09817
Ag	3.91473	1.7752	0.06288
Ag	3.49623	-2.50079	-0.06087
Ag	3.10103	-0.28937	-2.01649
H	-1.70998	-4.42777	4.7722
H	-2.49077	-2.38039	4.88801
H	3.29255	-0.97128	4.88739
H	4.68183	0.72396	4.78077
H	3.32988	-7.00641	1.8356
H	3.04516	-6.07715	-0.12847
H	6.78576	-0.40289	0.12876

H	7.73248	-0.62054	-1.83548
H	4.40374	6.38726	1.82206
H	3.73747	5.66517	-0.1369
H	-2.96953	3.69516	4.77881
H	-0.80683	3.33924	4.88544
P	-1.56271	-3.16084	4.14655
P	3.51138	0.22381	4.14979
P	2.66998	-5.90274	1.23147
P	6.4468	-0.64006	-1.23119
P	3.77722	5.26045	1.22517
P	-1.95139	2.93096	4.14823
S	0.	0.	0.
S	-2.29656	-3.37385	2.24178
S	0.29705	-2.46166	4.49891
S	1.97927	1.48955	4.49921
S	4.06798	-0.30244	2.24576
S	0.69487	-6.14685	1.47262
S	3.58562	-4.22631	1.94368
S	5.67021	-2.4723	-1.47289
S	5.45322	0.99175	-1.94271
S	4.97719	3.67373	1.47214
S	1.86911	5.21788	1.94175
S	-2.28205	0.97158	4.49904
S	-1.774	3.67477	2.24369
Ag	0.41487	4.27826	-0.06021
Ag	-1.29939	2.83022	-2.0177
Pd	1.1809	1.64233	-1.09702
Ag	0.0021	0.00105	-3.31577
Pd	-2.01182	0.20188	-1.09866
Ag	-1.8009	-2.54032	-2.01628
Pd	0.83197	-1.84327	-1.09817
Ag	-3.91473	-1.7752	-0.06288
Ag	-3.49623	2.50079	0.06087
Ag	-3.10103	0.28937	2.01649

H	1.70998	4.42777	-4.7722
H	2.49077	2.38039	-4.88801
H	-3.29255	0.97128	-4.88739
H	-4.68183	-0.72396	-4.78077
H	-3.32988	7.00641	-1.8356
H	-3.04516	6.07715	0.12847
H	-6.78576	0.40289	-0.12876
H	-7.73248	0.62054	1.83548
H	-4.40374	-6.38726	-1.82206
H	-3.73747	-5.66517	0.1369
H	2.96953	-3.69516	-4.77881
H	0.80683	-3.33924	-4.88544
P	1.56271	3.16084	-4.14655
P	-3.51138	-0.22381	-4.14979
P	-2.66998	5.90274	-1.23147
P	-6.4468	0.64006	1.23119
P	-3.77722	-5.26045	-1.22517
P	1.95139	-2.93096	-4.14823
S	2.29656	3.37385	-2.24178
S	-0.29705	2.46166	-4.49891
S	-1.97927	-1.48955	-4.49921
S	-4.06798	0.30244	-2.24576
S	-0.69487	6.14685	-1.47262
S	-3.58562	4.22631	-1.94368
S	-5.67021	2.4723	1.47289
S	-5.45322	-0.99175	1.94271
S	-4.97719	-3.67373	-1.47214
S	-1.86911	-5.21788	-1.94175
S	2.28205	-0.97158	-4.49904
S	1.774	-3.67477	-2.24369